University of Nebraska - Lincoln

DigitalCommons@University of Nebraska - Lincoln

2009

Output Maximization Control for DFIG Wind Turbines without Using Wind and Shaft Speed Measurements

Wei Qiao
University of Nebraska–Lincoln, wqiao@engr.unl.edu

Xiang Gong
University of Nebraska–Lincoln

Liyan Qu
University of Nebraska-Lincoln, lqu2@unl.edu

Output Maximization Control for DFIG Wind Turbines without Using Wind and Shaft Speed Measurements

Wei Qiao
Member, IEEE
Department of Electrical Engineering
University of Nebraska–Lincoln
Lincoln, NE 68588-0511, USA
wqiao@engr.unl.edu

Xiang Gong
Student Member, IEEE
Department of Electrical Engineering
University of Nebraska–Lincoln
Lincoln, NE 68588-0511, USA

Liyan Qu
Member, IEEE
liyanqu@ieee.org

Abstract -- **Wind turbine generators (WTGs) are usually equipped with mechanical sensors to measure wind speed and turbine shaft rotating speed for system monitoring, control, and protection. The use of these sensors increases the cost and hardware complexity and reduces the reliability of the WTG system. This paper proposes a novel real-time speed estimation algorithm for wind turbines equipped with doubly-fed induction generators (DFIGs). In the proposed algorithm, both the wind and turbine shaft speeds are estimated from the measured DFIG output electrical power. The estimated speeds are then used to determine the maximum power point of the DFIG wind turbine. A P-Q decoupled control strategy is developed to continuously regulate the DFIG at the maximum power point without the need of using any wind or turbine shaft speed sensors.**

Index Terms--**Doubly-fed induction generator; maximum power generation; real-time speed estimation; sensorless control; wind turbine.**

I. INTRODUCTION

Wind power is capable of becoming a major contributor to the nation's and world's electricity supply over the next three decades [1]-[3]. Currently, the majority of large- and medium-size wind turbines are equipped with doubly-fed induction generators (DFIGs). Monitoring, control, and protection of wind turbine generators (WTGs) require the information of wind speed and turbine shaft speed, which are usually measured by well-calibrated professional mechanical sensors. In order to maintain these sensors in good operating condition, regular inspection and maintenance are required. Obviously, the use of these sensors increases both the equipment and maintenance costs of the WTG system. Moreover, the sensors are inevitably subject to failure even with careful maintenance. Sensor failure may further cause the failure of the WTG control and electrical systems [4]. According to the statistical data reported in [4], sensor failures constitute more than 14% of failures in WTG systems, while more than 40% of failures are linked to the failure of sensors, the control system, or the electrical system. Repairing the failed components requires additional cost and causes significant downtime resulting in a significant loss in electrical power production. Therefore, the use of sensors reduces the reliability and increases the operational cost of the WTG systems. In addition, wind speed sensors, such as

anemometers, are very sensitive to icing. In many locations that have excellent wind resources but long winters, special models of anemometers with electrically heated shaft and cups are required. Consequently, additional sensors and an electrical grid connection are required to measure the temperature and to run the heater, respectively.

The problems incurred in using wind and shaft speed sensors can be solved through mechanical sensorless control. Previous research has focused on three types of sensorless control for WTG systems, namely, power signal feedback (PSF) [5]-[8], hill-climb searching (HCS) [9]-[11], and wind speed prediction [12]. In PSF control, wind speed is estimated using the measured WTG power and shaft speed based on the knowledge of the WTG power characteristics. The HCS method searches for the optimal operating point of WTGs through an incremental control action. Based on performance comparison of the WTG system at the present and previous time steps, the controller incrementally increases, decreases, or fixes the control variables to achieve the optimal operating point of the system. Theoretically, this method needs neither wind speed and turbine shaft speed nor knowledge of wind turbine characteristics. However, the HCS control works well only when the wind turbine inertia is very small, so the turbine speed reacts to wind speed almost instantaneously, which is generally not true for most DFIG wind turbines. Moreover, if the wind speed changes significantly from moment to moment, this method may never be able to locate the optimal operating point because of the long search time requirement. In a wind-speed-prediction-based control, an autoregressive statistical model is developed to predict the wind speed from the historical data. Therefore, this method does not need the information of the turbine shaft speed. However, this method may result in a complex computation, and the predicted wind speed is not accurate for real-time control of WTG systems.

This paper extends the work in [5] by proposing a P-Q decoupled output maximization control for DFIG wind turbines. A real-time speed estimation algorithm is developed where both the wind and turbine shaft speeds are estimated from the measured generator output electrical power, based on the knowledge of the WTG dynamics and power characteristics. The estimated wind and turbine shaft speeds are then used to determine the optimal power references for
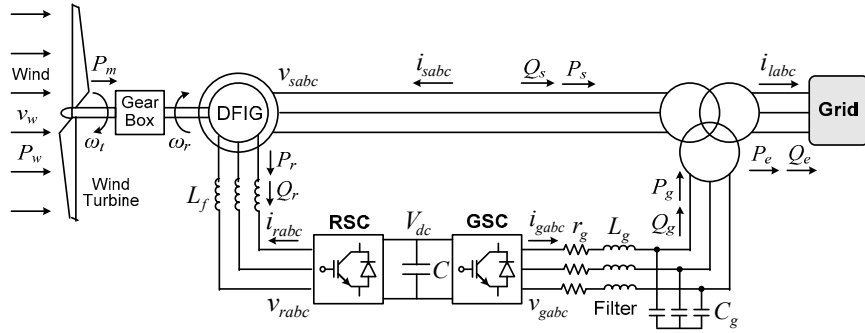
Fig. 1. Configuration of a DFIG wind turbine connected to a power grid.

controlling the DFIG wind turbine. Consequently, the WTG is optimally controlled to generate the maximum electrical power without the need of using any wind or turbine shaft speed sensors.

II. DFIG WIND TURBINE SYSTEM

Fig. 1 illustrates the basic configuration of a DFIG wind turbine. It consists of a low-speed wind turbine driving a high-speed DFIG through a gearbox. The DFIG is a wound-rotor induction machine. It is connected to a power grid at both stator and rotor terminals. The stator is directly connected to the grid while the rotor is fed through a variable frequency dc-link-voltage converter, which consists of a rotor-side converter (RSC) and a grid-side converter (GSC) and usually has a rating of a fraction (25%-30%) of the DFIG nominal power. As a consequence, the WTG can operate with the rotational speed in a range of ±25%-30% around the synchronous speed, and its active and reactive power can be controlled independently. Typically this type of wind turbine is also equipped with a blade pitch control to limit the extracted power during conditions of high wind speeds.

III. REAL-TIME WIND SPEED ESTIMATION

For a WTG system, the electrical power generation from wind energy can be described by the mathematical models in the flow chart in Fig. 2. The conversion of wind energy (P_w) to turbine mechanical power (P_m) is represented by a wind turbine aerodynamic model. In this model, the turbine mechanical power P_m is represented as a nonlinear function of the wind speed v_w, turbine shaft speed ω_t, and blade pitch angle β. The dynamics of the WTG shaft system is represented by a set of differential equations. Consequently, the mechanical power is transferred from the turbine to the generator (P_{in}). The generator converts mechanical power into electrical power (P_e), where $P_e = P_s + P_r$ (see Fig. 1). The losses (P_{loss}) of the system (referred to the generator side) are considered in the model. The output electrical power P_e of the generator is measured. Therefore, if developing an inverse model from P_e to v_w, then the wind speed can be estimated from the measured output electrical power.
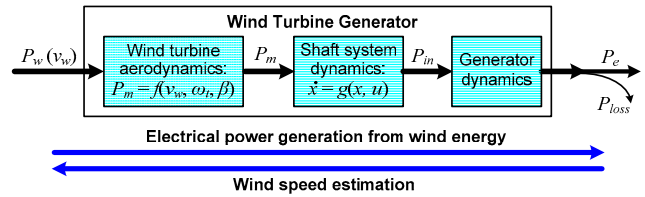

Fig. 2. The principle of wind speed estimation.

In the proposed algorithm, the wind speed v_w is estimated directly from the nonlinear inverse mapping of the wind turbine aerodynamics, provided that values are known for P_m, ω_t, and β. In this work, both P_m and ω_t are estimated instead of being measured from sensors. The proposed algorithm then uses a three-layer Gaussian radial basis function network (GRBFN) to perform a static nonlinear inverse mapping of the wind turbine aerodynamics to estimate the wind speed, as shown in Fig. 3, where $\hat{v}_w$, $\hat{P}_m$, and $\hat{\omega}_t$ are the estimated values of v_w, P_m, and ω_t, respectively.

The GRBFN has been shown to be a universal approximator [13] for nonlinear functions. The overall input-output mapping for the GRBFN is given by:

$$\hat{v}_w = b + \sum_{j=1}^{h} v_j \exp\left(-\frac{\left\| x - C_j \right\|^2}{\sigma_j^2} \right) \tag{1}$$

where $x = [\hat{P}_m, \hat{\omega}_t, \beta]$ is the input vector; $C_j \in R^n$ and $\sigma_j \in R$ are the center and width of the jth RBF units in the hidden layer, respectively; h is the number of RBF units; b and v_j are the bias term and the weight between hidden and output layers, respectively; and $\hat{v}_w$ is the output of the GRBFN that represents the estimated wind speed.

The parameters of the GRBFN, including the number of RBF units, the RBF centers and width, and the output weights and bias term, are determined by using a training data set generated from the wind turbine aerodynamic characteristics This data set covers the entire operating range of the wind turbine [5]. The wind turbine aerodynamic characteristics are usually available from the turbine

manufacture. Once trained, the parameters of the GRBFN are then fixed for online estimation of the wind speed. Since the training data set covers the entire operating range of the wind turbine, the resulting GRBFN provides an accurate wind speed estimation model over the entire WTG operating range, provided that the values of P_m, and ω_t are estimated accurately.
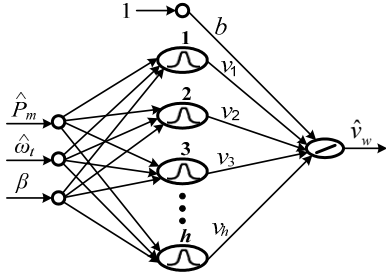

Fig. 3. GRBFN-based wind speed estimation algorithm.

IV. REAL-TIME TURBINE MECHANICAL POWER ESTIMATION

The turbine mechanical power P_m is estimated from the measured generator output electrical power P_e while taking into account the power losses and shaft system dynamics of the WTG. In this work, the shaft system of the WTG is simply modeled as a single lumped-mass system, given by:

$$2H_m \frac{d\omega_m}{dt} = \frac{P_m}{\omega_m} - \frac{P_e + P_{loss}}{\omega_m} - D_m \omega_m \tag{2}$$

where H_m is the lumped inertia constant of the system; ω_m is the shaft speed of the lumped-mass system and $\omega_m = \omega_t = \omega_r$ (see Fig. 1); D_m is the damping coefficient of the lumped-mass system; and the total power losses P_{loss} of the WTG system is calculated by the procedure given in [5]. In this paper, all quantities are expressed as per-unit values. Rewriting (2) in discrete-time format gives:

$$\hat{P}_m(t) = \left(\frac{2H_m}{\Delta t} + D_m\right)\hat{\omega}_m^2(t) - \frac{2H_m}{\Delta t}\hat{\omega}_m(t)\hat{\omega}_m(t-1) + P_e(t) + P_{loss}(t) \tag{3}$$

Equation (3) estimates P_m at any time step from the measured P_e and the estimated P_{loss}, provided that values are known for ω_m (estimated).

V. REAL-TIME TURBINE SHAFT SPEED ESTIMATION

In terms of the instantaneous variables shown in Fig. 1, the stator active power can be written in synchronously rotating dq reference frame as follows.

$$P_s = -\frac{3}{2}(v_{ds}i_{ds} + v_{qs}i_{qs}) \approx -\frac{3}{2}[\omega_s L_m(i_{qs}i_{dr} + i_{ds}i_{qr}) + r_s(i_{ds}^2 + i_{qs}^2)] \tag{4}$$

where ω_s is the rotational speed of the synchronous reference frame; r_s and L_m are the stator resistance and mutual inductance, respectively. Similarly, the rotor active power is calculated by:

$$P_r = -\frac{3}{2}(v_{dr}i_{dr} + v_{qr}i_{qr}) \approx \frac{3}{2}[s\omega_s L_m(i_{qs}i_{dr} + i_{ds}i_{qr}) - r_r(i_{dr}^2 + i_{qr}^2)] \tag{5}$$

where $s\omega_s$ is the slip frequency defined by $s\omega_s = \omega_s - \omega_r$; ω_r is the rotor speed. Equations (4) and (5) yield

$$s = -\frac{P_r + \frac{3}{2}r_r(i_{dr}^2 + i_{qr}^2)}{P_s + \frac{3}{2}r_s(i_{ds}^2 + i_{qs}^2)} = -\frac{P_r + 3i_r^2 r_r}{P_s + 3i_s^2 r_s} \tag{6}$$

Consequently, the DFIG rotor speed ω_r can be estimated as:

$$\hat{\omega}_r = (1-s)\omega_s = \left[1 + \frac{P_r + 3i_r^2 r_r}{P_s + 3i_s^2 r_s}\right]\omega_s \tag{7}$$

where $\hat{\omega}_r$ is the estimated value of ω_r. In a DFIG wind turbine, the three-phase stator and rotor voltages and currents are usually measured for system monitoring, control, and protection. Consequently, the stator power P_s and rotor power P_r can be calculated. Assume the grid frequency f_s is constant at 60 Hz, therefore, $\omega_s = 2\pi f_s$ is a constant. According to (7), the DFIG rotor speed ω_r can be estimated from the measured electrical quantities of the DFIG only. Therefore, the WTG shaft speed ω_m is estimated as $\hat{\omega}_m = \hat{\omega}_r$ based on the lumped-shaft model (2).

VI. MECHANICAL SPEED-SENSORLESS CONTROL FOR DFIG WIND TURBINES

The mechanical power that a wind turbine extracts from wind can be calculated by:

$$P_m = \frac{1}{2}\rho A_r v_w^3 C_P(\lambda, \beta) \tag{8}$$

where ρ is the air density; $A_r = \pi R^2$ is the area swept by the rotor blades; C_P is the power coefficient, which is a function of both tip speed ratio λ and the blade pitch angle β; and λ is defined by $\lambda = \omega_t R/v_w$, where R is the wind turbine rotor radius. For any wind turbine there is an optimal tip speed ratio λ_{opt} (a constant) which yields the maximum power coefficient C_{Pm} at any wind speed within the operating range. According to (8), when C_P is controlled at the maximum value, the wind turbine extracts the maximum mechanical power and, consequently, the DFIG generates the maximum electrical power from the wind. At this optimal condition, based on the estimated wind speed $\hat{v}_w$, the corresponding maximum mechanical power $P_{m,max}$ of the wind turbine can be calculated as:

$$P_{m,max} = \frac{1}{2}\rho A_r \hat{v}_w^3 C_{Pm}(\lambda_{opt}, \beta) \tag{9}$$

Based on (2), (3) and (9), the maximum DFIG output electrical power $\hat{P}_{e,max}$ at each time step can be estimated by:

$$\hat{P}_{e,max}(t) = P_{m,max}(t) - D_m \omega_{t,opt}^2(t) - P_{loss}(t) - H_m \frac{d\omega_{t,opt}^2(t)}{dt} \tag{10}$$

$$\approx P_{m,max}(t) - D_m \omega_{t,opt}^2(t) - P_{loss}(t)$$

where $\omega_{t,opt} = \lambda_{opt}\hat{v}_w/R$ is the optimal turbine shaft speed corresponding to the maximum power point and $P_{loss}(t)$ is the
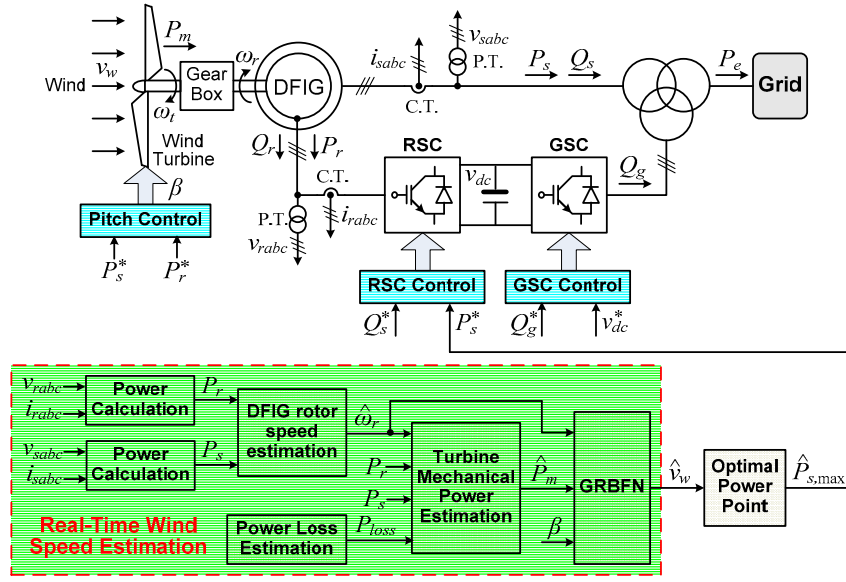
Fig. 4. Mechanical-speed-sensorless control for DFIG wind turbine to generate maximum electrical power.

power losses of the WTG.

According to (7) and (10), the maximum stator active power $\hat{P}_{s,max}$ can be estimated by:

$$\hat{P}_{s,max}(t) = \frac{\omega_s(t)}{\omega_{t,opt}(t)}\left[P_{e,max}(t) + 3i_s^2(t)r_s + 3i_r^2(t)r_r\right] - 3i_s^2(t)r_s$$

$$\approx \frac{\omega_s(t)}{\omega_{t,opt}(t)}P_{e,max}(t) \tag{11}$$

The $\hat{P}_{s,max}$ is then used by the RSC controller as the optimal stator active power reference (i.e., $P_s^* = \hat{P}_{s,max}$) for maximum power point tracking (MPPT). The overall control system of the WTG does not need any mechanical wind and turbine shaft speed sensors.

The proposed real-time wind speed estimation algorithm is integrated into the control system of the DFIG wind turbine, as shown in Fig. 4. The DFIG wind turbine control system generally consists of two parts: the electrical control of the DFIG and the mechanical control of the wind turbine blade pitch angle. Control of the DFIG is achieved by controlling the RSC and the GSC. The control objective of the RSC is to regulate both the stator-side active and reactive power independently. The control objective of the GSC is to keep the dc-link voltage constant regardless of the magnitude and direction of the rotor power. The GSC control scheme can also be designed to regulate the reactive power of the DFIG. The blade pitch angle control regulates the pitch angles of the wind turbine blades, which determines the mechanical power that the turbine extracts from the wind. The blade pitch angle control is only activated when the wind speed is higher than the rated value. The details of the DFIG wind turbine control system are given in [14].

Fig. 5 illustrates the schematic diagram of the overall close-loop WTG system, including the wind speed estimation algorithm and the WTG controller. Since the wind speed usually varies fast but the response of the WTG is relatively slow due to its inertia, the possible high-frequency, i.e., the frequency higher than the self-excitation frequency of the open-loop system in Fig. 5, components in the optimal power reference signals may cause self-excitation of the system. To achieve a stable MPPT control, a low-pass filter is required to attenuate the open-loop gain of the system at the self-excitation frequency. In this paper, a forth-order, low-pass filter is used to eliminate the possible self-excitation of the system. The cut-off frequency of the low-pass filter is 0.7 Hz, which is less than the self-excitation frequency of 1.4 Hz of the open-loop WTG system.
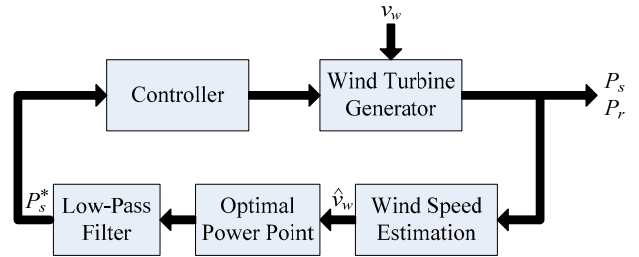

Fig. 5. Schematic diagram of the overall close-loop WTG system, including the wind speed estimation algorithm and WTG controller.

VII.   SIMULATION RESULTS

Simulation studies are carried out in PSCAD/EMTDC for a 3.6-MW DFIG wind turbine [5] to verify the effectiveness of the proposed real-time speed estimation algorithm and

sensorless control strategy. Some typical results are demonstrated and discussed in this section.

A. Maximum Power Generation during Wind Speed Variations

The wind speed varies in a range of ±3 m/s around the mean value of 12 m/s, as shown in Fig. 6. The wind speed variations cause variations of the WTG mechanical and electrical quantities, such as the turbine mechanical power, shaft speeds, electrical power, etc. Figs. 6-8 compare the actual and estimated wind speeds, the actual and estimated DFIG shaft speeds, and the actual and estimated turbine mechanical powers, respectively. These results show that the proposed algorithm accurately estimates the DFIG shaft speed and turbine mechanical power. Consequently, the wind speed is accurately estimated in real time.

Based on the estimated wind and turbine shaft speeds, the optimal DFIG stator active power reference is determined for maximum electrical power generation. Fig. 9 shows the reference and actual values of the DFIG stator active power. The stator active power is well controlled by the DFIG controllers to track the optimal reference with a good precision during wind speed variations. Consequently, the WTG continuously generates the maximum electrical power, as shown in Fig. 10. This maximum power generation can be demonstrated by the result of the wind turbine tip speed ratio, as shown in Fig. 11. The actual tip speed ratio varies in a small range around the average value of 5.95. The variations of the tip speed ratio are caused by fast variations of the wind speed and the relatively slow responses of the WTG system. However, the average tip speed ratio is almost the same as the optimal tip speed ratio of λ_{opt} = 5.96.
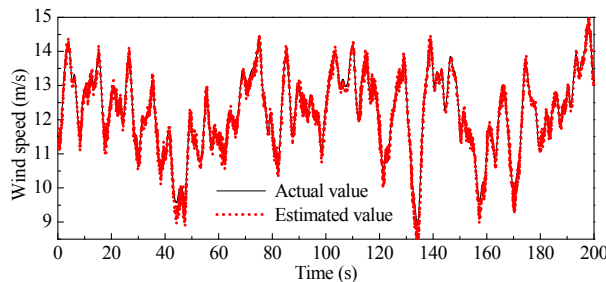

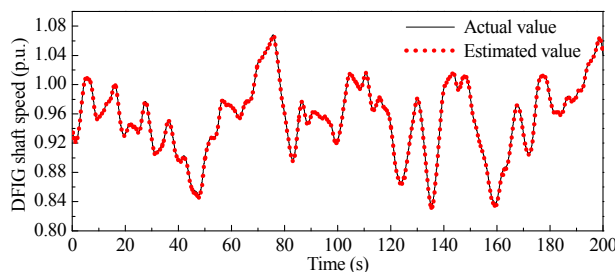Fig. 6. MPPT: wind speed estimation results.

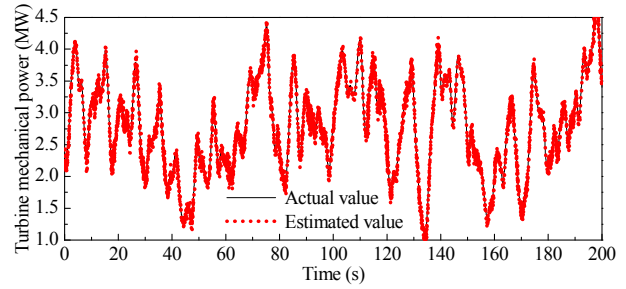Fig. 7. MPPT: DFIG shaft speed estimation results.

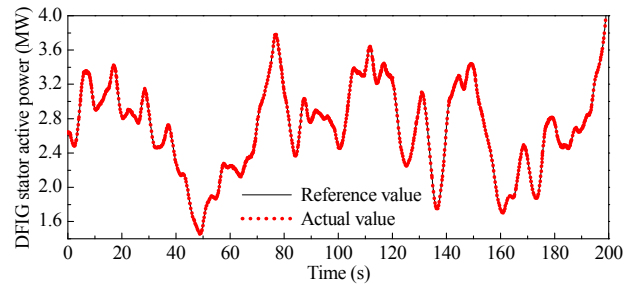Fig. 8. MPPT: wind turbine mechanical power estimation results.

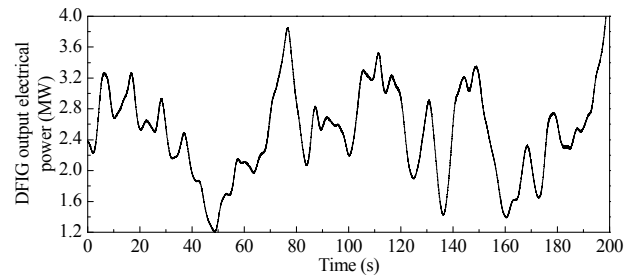Fig. 9. MPPT: FDIG stator active power tracking results.

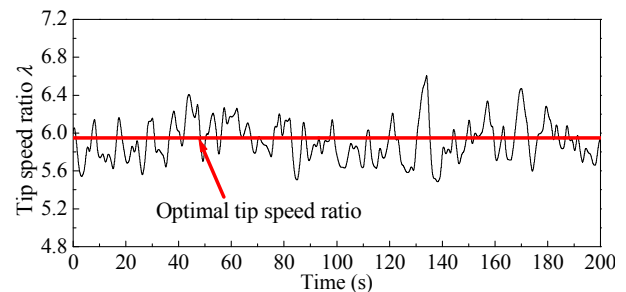Fig. 10. MPPT: output electrical power of the DFIG.

Fig. 11. MPPT: actual and optimal tip speed ratios.

B. Constant Power Generation during Wind Speed Variations

With the same wind conditions as in Section VII-A, the DFIG stator active power reference is now maintained at a constant value of 2.56 MW during wind speed variations. The corresponding results are shown in Figs. 12-15. The stator active power is well controlled by the DFIG controllers at the constant value of 2.56 MW even when the wind speed

varies significantly, as shown in Fig. 12. Again, the proposed algorithm accurately estimates the DFIG shaft speed (Fig. 13) and turbine mechanical power (Fig. 14). Consequently, the wind speed is accurately estimated in real time (Fig. 15). Compared to Fig. 9, the DFIG shaft speed varies in a large range since the DFIG is not controlled optimally to generate the maximum electrical power.
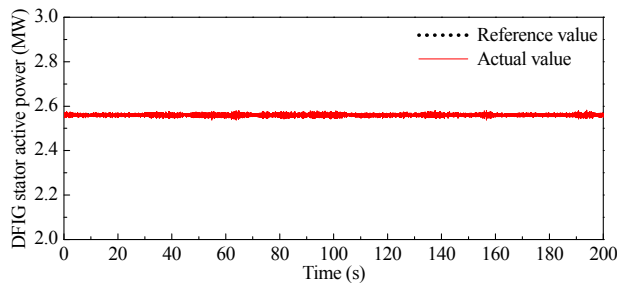

Fig. 12. Constant power control: FDIG stator active power tracking results.
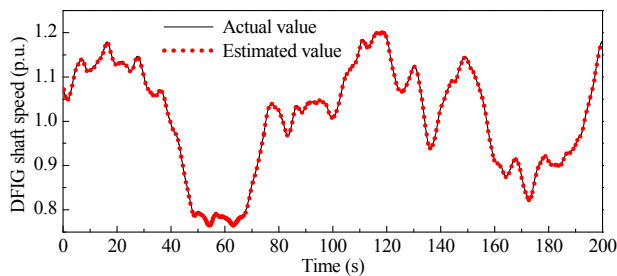

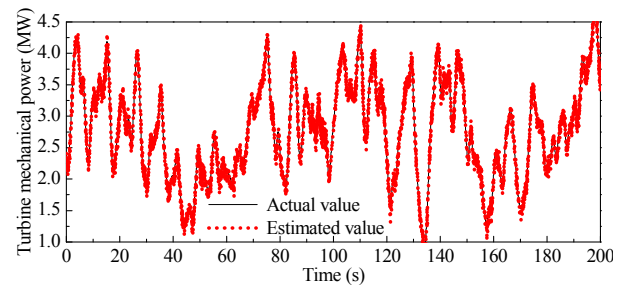Fig. 13. Constant power control: DFIG shaft speed estimation results.

Fig. 14. Constant power control: wind turbine mechanical power estimation results.
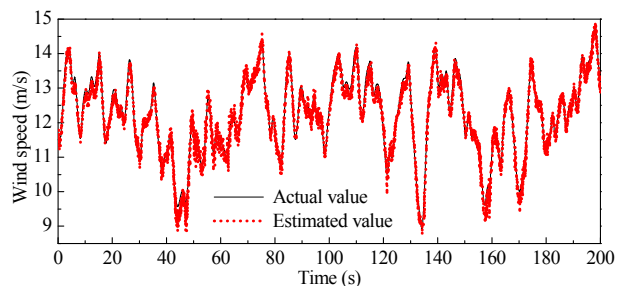

Fig. 15. Constant power control: wind speed estimation results.

C. Grid Fault during Wind Speed Variations

With the same wind conditions as in Section VII-A, the DFIG is again optimally controlled to generate the maximum electrical power. At 10 s, a 200-ms temporary three-phase short circuit is applied to the grid close to the terminal of the DFIG. This grid fault causes a 200-ms voltage dip at the terminal of the DFIG (Fig. 16) and a short period of transient in the WTG mechanical and electrical quantities, as shown in Figs. 17-20. Except for the short period of the transient state following the grid fault, the proposed algorithm accurately estimates the DFIG shaft speed (Fig. 17) and turbine mechanical power (Fig. 18) and consequently the wind speed (Fig. 19) in real time. These results show that the proposed algorithm can ride through grid faults to continuously provide accurate speed estimation. The performance degradation of the speed estimation algorithm during the transient state does not affect the performance of the WTG controllers, as shown in Fig. 20. The proposed mechanical-speed-sensorless control strategy works well at various operating conditions, including the most challenging operating conditions, i.e., the grid fault conditions.
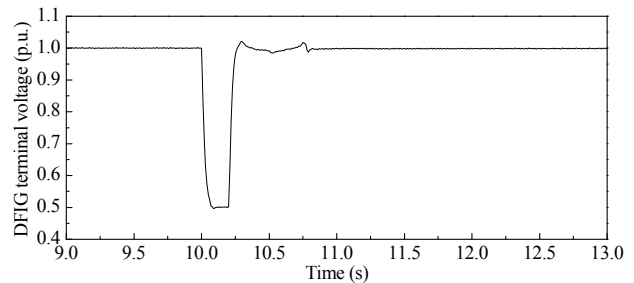

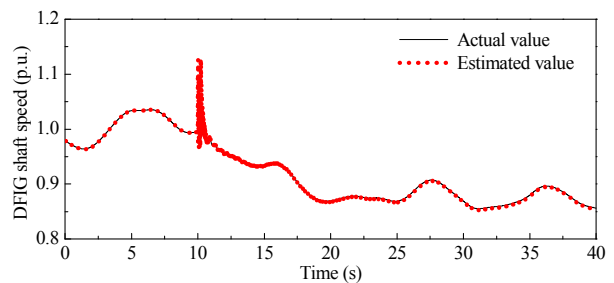Fig. 16. Grid fault: DFIG terminal voltage.

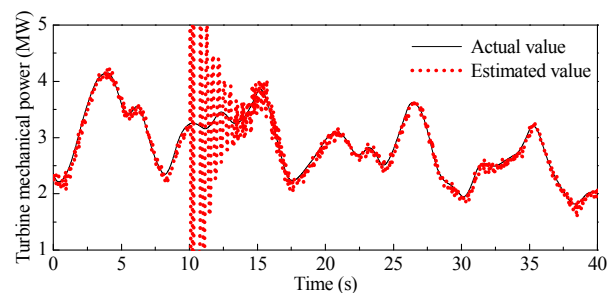Fig. 17. Grid fault: DFIG shaft speed estimation results.

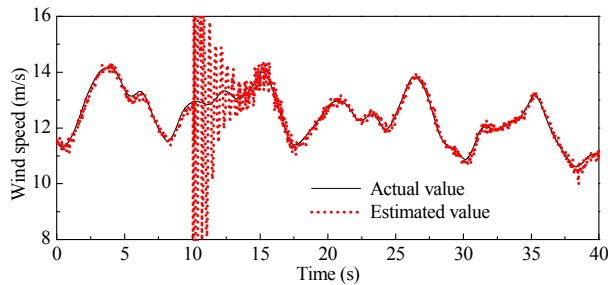Fig. 18. Grid fault: wind turbine mechanical power estimation results.

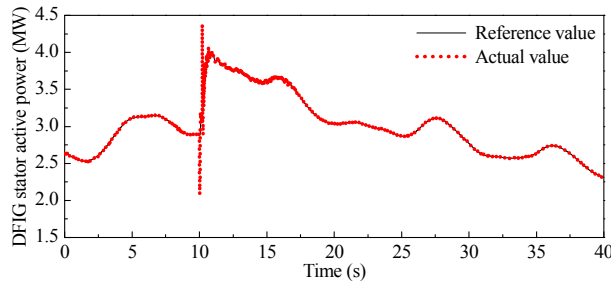Fig. 19. Grid fault: wind speed estimation results.

Fig. 20. Grid fault: FDIG stator active power tracking results.

VIII. CONCLUSIONS

This paper has proposed a novel mechanical-speed-sensorless control for maximum wind power generation using DFIG wind turbines. A real-time speed estimation algorithm has been developed to estimate both the wind and turbine shaft speeds from the measured DFIG output electrical powers. The estimated speeds are then used to determine the maximum power point for the DFIG controller to generate the maximum electrical power from the wind. The performance of the proposed real-time speed estimation algorithm and sensorless control strategy has been evaluated by simulation studies for a 3.6-MW DFIG wind turbine. Results have shown that the proposed speed estimation and sensorless control algorithms work well at various operating conditions.

REFERENCES

[1] "Global wind energy outlook 2008", Global Wind Energy Council, Oct. 2008 (available online: http://www.gwec.net/index.php?id=92).
[2] "20% wind energy by 2030: Increasing wind energy's contribution to U.S. electricity supply," U.S. Department of Energy, July 2008.
[3] "Focus on 2030: EWEA aims for 22% of Europe's electricity by 2030," *Wind Directions*, pp. 25-34, Nov./Dec. 2006.
[4] J. Ribrant and L. M. Bertling, "Survey of failures in wind power systems with focus on Swedish wind power plants during 1997-2005," *IEEE Trans. Energy Conversion*, vol. 22, no. 1, pp. 167-173, Mar. 2007.
[5] W. Qiao, W. Zhou, J. M. Aller, and R. G. Harley, "Wind speed estimation based sensorless output maximization control for a wind turbine driving a DFIG," *IEEE Trans. Power Electronics*, vol. 23, no. 3, pp. 1156-1169, May 2008.
[6] H. Li, K. L. Shi, and P. G. McLaren, "Neural-network-based sensorless maximum wind energy capture with compensated power coefficient," *IEEE Tran. Industry Applications*, vol. 41, no. 6, pp. 1548-1556, Nov./Dec. 2005.

[7] B. Boukhezzar and H. Siguerdidjane, "Nonlinear control of variable speed wind turbines without wind speed measurement," in *Proc. 44th IEEE Conference on Decision and Control*, Seville, Spain, Dec. 12-15, 2005, pp. 3456-3461.
[8] S. Bhowmik, R. Spee, and J. H. R. Enslin, "Performance optimization for doubly fed wind power generation systems," *IEEE Trans. Industry Applications*, vol. 35, no. 4, pp. 949-958, Jul./Aug. 1999.
[9] T. Tanaka and T. Toumiya, "Output control by Hill-Climbing method for a small wind power generating system," *Renewable Energy*, vol. 12, no. 4, pp. 387-400, 1997.
[10] M. G. Simoes, B. K. Bose, and R. J. Spiegel, "Fuzzy logic based intelligent control of a variable speed cage machine wind generation system," *IEEE Trans. Power Electronics*, vol. 12, no. 1, pp. 87-95, Jul./Aug. 1997.
[11] Q. Wang and L. Chang, "An intelligent maximum power extraction algorithm for inverter-based variable speed wind turbine systems," *IEEE Trans. Power Electronics*, vol. 19, no. 5, pp. 1242-1249, Sept. 2004.
[12] K. Tan and S. Islam, "Optimal control strategies in energy conversion of PMSG wind turbine system without mechanical sensors," IEEE Trans. Energy Conversion, vol. 19, no. 2, pp. 392-399, Jun. 2004.
[13] J. Park and I. W. Sandberg,, "Universal approximation using radial-basis-function networks," *Neural Computation*, vol. 3, no. 3, pp. 246-257, 1991.
[14] W. Qiao, "Dynamic modeling and control of doubly fed induction generators driven by wind turbines," in *Proc. 2009 IEEE PES Power Systems Conference & Exposition*, Seattle, WA, USA, Mar. 15-18, 2009.